J|A|C|S
ARTICLES
Published on Web 04/23/2005

Picosecond Dynamics of Nonthermalized Excited States in Tris(2,2-bipyridine)ruthenium(II) Derivatives Elucidated by High Energy Excitation

Sherri A. McFarland,* Felix S. Lee, Karen A. W. Y. Cheng, Frances L. Cozens, and Norman P. Schepp*

Contribution from the Department of Chemistry, Dalhousie University, Halifax, NS B3H 4J3, Canada

Received June 28, 2004; Revised Manuscript Received March 8, 2005; E-mail: sherri.mcfarland@dal.ca; norman.schepp@dal.ca

Abstract: The picosecond excited-state dynamics of several derivatives have been investigated using high photon energy excitation combined with picosecond luminescence detection. Instrument response-limited fluorescence ($\tau_1 \approx 3-5$ ps) at 500 nm was observed for all of the complexes, while longer-lived emission ($\tau_2 > 50$ ps), similar in energy, was observed for only some of the complexes. Interestingly, the presence of τ_2 required substitution at the 4,4-positions of the bipyridine ligands and D_3 symmetry for the complex; only the 4,4-substituted homoleptic complexes exhibited τ_2. On the basis of previous assignments of the ultrafast dynamics measured for $Ru(bpy)_3^{2+}$ and $Ru(dmb)_3^{2+}$, τ_2 has been tentatively ascribed to relaxation from higher electronic or vibrational levels in the triplet manifold having slightly more triplet character than the state responsible for τ_1. However, given that the kinetics for these transition metal complexes are highly dependent on both pump and probe wavelengths and that there is considerable interest in utilizing such complexes for electron transfer in the nonergodic limit, further characterization of the state giving rise to τ_2 is warranted.

1. Introduction

The underlying mechanism for the conversion of light into energy is charge separation. At the molecular level, this separation involves absorption of a photon and subsequent charge redistribution in the molecule. The maintenance and/or amplification of the resulting chemical potential is determined by the chain of events that immediately follows photon absorption. Therefore, the study of charge transfer and its role in achieving efficient solar energy conversion relies on the knowledge of the factors affecting these early photophysical processes. Transition metal complexes, namely ruthenium polypyridyl complexes, have long served as the prototype for such investigations,[1−3] and accordingly, their lowest-energy excited states are well-characterized.[4−9] However, minimal radiative coupling to the ground state often prevents direct access to these low-energy states, and higher-energy excited states must be populated to gain access to the emissive states. It is the photophysical dynamics involving these nonthermalized states that have been the focus of recent work in several laboratories.[10−13] In particular, it has been reported recently that the rate of electron injection from $Ru(dcbpy)_2(NCS)_2$ to TiO_2, a fundamental aspect of sensitization in wide band gap semiconductors, is strongly dependent on excitation wavelength, which determines the nature of the initially populated vibronic hot state.[14] Simplistically, the higher the state, the faster the electron injection; therefore, solar energy conversion in these devices is most efficient when operating in the nonergodic limit.[15] This observation, in addition to recent reports of singlet emission in $Ru(bpy)_3^{2+}$,[12,13] led us to examine the picosecond dynamics of nonthermalized excited states in a series of derivatives using high-energy excitation.

It has been determined that the absorptive properties of the thermalized ^{3}MLCT state of $Ru(bpy)_3^{2+}$ are established within 300 fs ($\lambda_{ex} = 480$ nm)[10] while the rate constant for intersystem crossing (ISC) is ~40 fs, indicating that ISC originates from the Franck−Condon state.[12] The discrepancy between the evolution of the singlet wave packet and the time scale for thermalized ^{3}MLCT state formation is thought to arise as a result

(1) Wishart, J. F., Nocera, D. G., Eds.; *Photochemistry and Radiation Chemistry: Complementary Methods for the Study of Electron Transfer*; ACS Advances in Chemistry Series 254; American Chemical Society: Washington, DC, 1998.
(2) Kalyanasundaram, K.; Gratzel, M. *Coord. Chem. Rev.* **1998**, *177*, 347−414.
(3) Balzani, V.; Credi, A.; Scanola, F. *NATO ASI Ser., Ser. C* **1994**, *36*, 1−32.
(4) Kalyanasundaram, K. *Coord. Chem. Rev.* **1982**, *46*, 159−244.
(5) Juris, A.; Barigelletti, F.; Balzani, V.; Belser, P.; Zelewsky, A. V. *Inorg. Chem.* **1985**, *24*, 202−206.
(6) Meyer, T. *Pure Appl. Chem.* **1986**, *58*, 1193−1200.
(7) Juris, A.; Balzani, V.; Barigelletti, F.; Campagna, S.; Belser, P.; Zelewsky, A. V. *Coord. Chem. Rev.* **1988**, *84*, 85−277.
(8) Balzani, V.; Barigelletti, F.; Cola, L. *Top. Curr. Chem.* **1990**, *158*, 31−74.
(9) Kalyanasundaram, K. *Photochemistry of Polypyridine and Porphyrin Complexes*; Academic Press: San Diego, CA, 1992.
(10) Damrauer, N. H.; Cerullo, G.; Yeh, A.; Boussie, T. R.; Shank, C. V.; McCusker, J. K. *Science* **1997**, *275*, 54−57.
(11) Yeh, A. T.; Shank, C. V.; McCusker, J. K. *Science* **2000**, *289*, 935−938.
(12) Bhasikuttan, A. C.; Suzuki, M.; Nakeshima, S.; Okada, T. *J. Am. Chem. Soc.* **2002**, *124*, 8398−8405.
(13) Browne, W. R.; Coates, C. G.; Brady, C.; Matousek, P.; Towrie, M.; Botchway, S. W.; Parker, A. W.; Vos, J. G.; McGarvey, J. J. *J. Am. Chem. Soc.* **2003**, *125*, 1706−1707.
(14) Benko, G.; Kallioinen, J.; Korppi-Tommola, J. E. I.; Yartsev, A. P.; Sundstrom, V. *J. Am. Chem. Soc.* **2002**, *124*, 489−493.
(15) Bernstein, R. B.; Zewail, A. H. *J. Phys. Chem.* **1986**, *90*, 3467−3469.

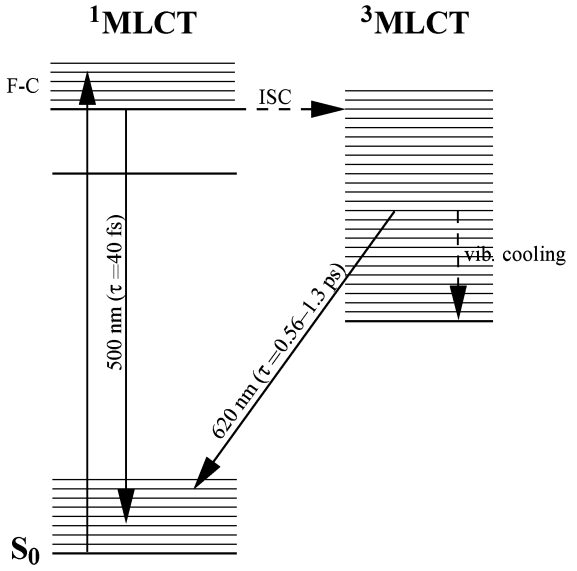

Figure 1. Proposed model for nonthermalized excited-state decay in $Ru(bpy)_3^{2+}$.

of the slower time constant encompassing a host of dynamic processes including ISC, internal conversion (IC), charge localization, vibrational relaxation, and intramolecular vibrational energy redistribution (IVR). With this in mind, it is reasonable to assume that any photophysical process occurring with a half-life greater than ~40 fs is representative of triplet surface dynamics. Accordingly, the 600-fs component in the biexponential decay (575 nm) observed by Bhasikuttan et al. using fluorescence upconversion was assigned to vibrational cooling within the triplet manifold of $Ru(bpy)_3^{2+}$ (Figure 1).[12]

A model wherein ISC occurs much faster than vibrational cooling is unique to transition metal complexes. A simple cascade picture of excited-state evolution (where $k_{vib} \gg k_{IC} \gg k_{ISC}$), while useful in the interpretation of organic photophysics, does not adequately describe a system in which a large number of electronic and vibrational states can participate in excited state decay. Consequently, the relaxation pathway ultimately depends on the state(s) initially populated, resulting in a strong excitation-wavelength dependence for the observed kinetics.[16−18] Therefore, we set out to investigate the picosecond dynamics of a series of homo- and heteroleptic Ru(II) complexes (derived from the ligands shown in Chart 1) at shorter excitation wavelengths using a streak camera to detect luminescence from nonthermalized excited state(s).[19] The fundamental questions we wished to address include: (1) Does $Ru(bpy)_3^{2+}$ show luminescence from nonthermalized states on the picosecond time scale? (2) What are the picosecond dynamics exhibited by derivatives of $Ru(bpy)_3^{2+}$? (3) What are the effects of shorter wavelength excitation on these dynamics?

2. Experimental Section

Ruthenium(II) complexes based on the ligands shown in Chart 1 were synthesized according to modified literature protocols and characterized by TLC, ^{1}H NMR, ^{13}C NMR, and mass spectrometry

Chart 1. Bipyridyl Ligands

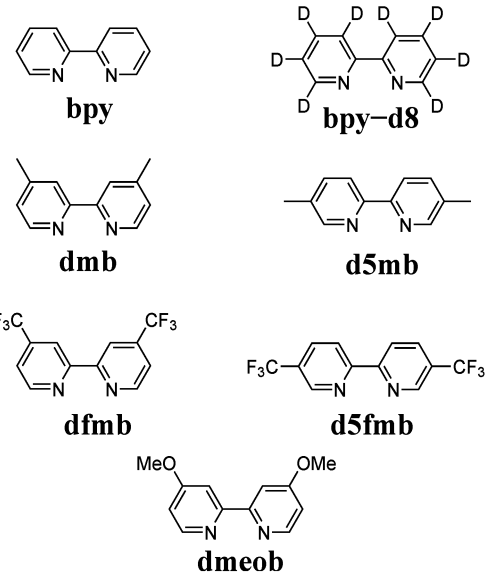

(see Supporting Information). In addition, steady-state absorption and emission measurements were carried out to establish the nature of the Franck−Condon state (^{1}MLCT) and the lowest-energy excited state (^{3}MLCT). The ^{3}MLCT-state lifetimes were determined by nanosecond time-resolved luminescence decay (~640 nm), and the ligand localizing the charge was identified by nanosecond transient absorption spectroscopy. All spectroscopic measurements were performed on the Cl_2 salts of the ruthenium(II) complexes in aqueous solutions and the corresponding $2{\cdot}PF_6$ salts in acetonitrile solutions, and where possible, the parameters obtained from static and nanosecond spectroscopies were compared to those in the literature.

Time-resolved luminescence measurements were performed using a Clark-MXR CPA-2001 femtosecond laser for sample excitation and a streak camera (Axis-Photonique) coupled to a CCD camera (SenSys) for detection. Briefly, the CPA-2001 employs an all solid-state diode-pumped Erbium-fiber laser that generates <150 fs, 775-nm pulses at 1 kHz with an output energy of ~800 μJ/pulse. These pulses are directed into a STORC-2001 unit (Clark-MXR) for separation; one of the pulses is frequency-doubled to 388 nm (or tripled to 258 nm) for sample excitation, and the unchanged fundamental is used to trigger the G2 Jitter-free Unit (Axis-Photonique), which produces the voltage ramp for the streak camera. The G2 Jitter-free Unit produces a time window of 340 ps with 3−5 ps resolution for front-face excitation of solution samples. For longer time windows, the streak camera is triggered electronically via a slow sweep unit, designed by Axis Photonique, Inc. and built by Kentech Instruments. The time windows available currently using the slow sweep unit are 4.3, 11.7, 27.9, and 92.6 ns with instrument response functions (IRF) fwhm of 64, 116, 180, and 750 ps, respectively.

Front-face excitation of the sample, contained in a 1.0-mm Helma quartz cell, produced emission that was collimated, passed through a 400-nm cutoff filter, and focused into the streak camera (operating at 1 kHz) through a 500-nm band-pass filter. Exposure times of 3−12 min produced images that were captured with a CCD camera (SenSys) using Photometrics IPLab software. These images were corrected for instrinsic curvature and tilt using software written in-house with LabVIEW 5.1 and summed vertically to yield kinetic information. The IRF was determined to be ~4−4.5 ps by measuring scatter of the incident laser light from a colloidal suspension of corn starch in H_2O. Kinetic fits of the experimental data convoluted with the IRF were calculated according to the Marquardt−Levenberg algorithm using LabVIEW software written in-house and evaluated on the basis of the pattern of residuals and reduced-χ^2 values.

(16) Farrell, I. R.; Matousek, P.; Towrie, M.; Parker, A. W.; Grills, D. C.; George, M. W.; Vicek, A., Jr. *Inorg. Chem.* **2002**, *41*, 4318−4323.
(17) Shiang, J. J.; Walker, L. A., II; Anderson, N. A.; Cole, A. G.; Sension, R. J. *J. Phys. Chem. B* **1999**, *103*, 10532−10539.
(18) McCusker, J. K. *Acc. Chem. Res.* **2003**, *36*, 876−887.
(19) In this context, *nonthermalized* refers to any state residing above the lowest energy ^{3}MLCT state.

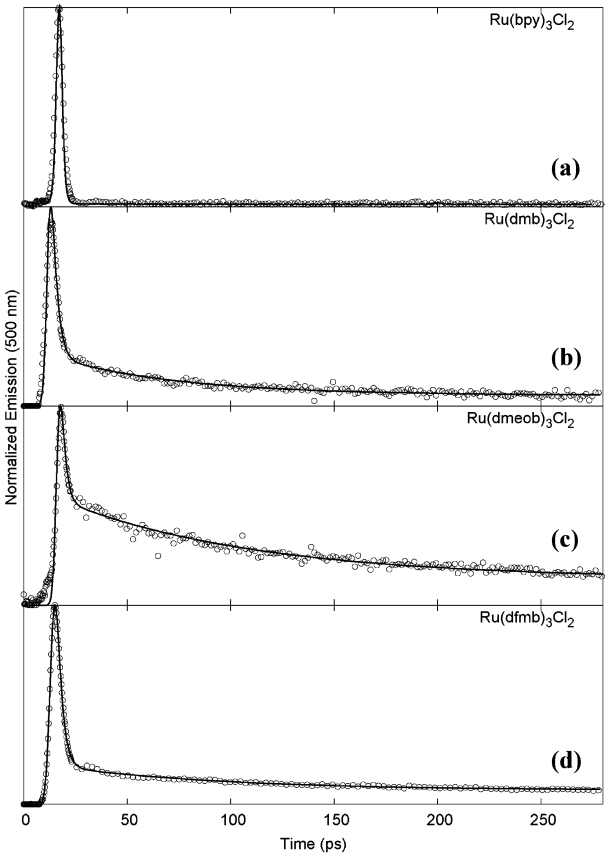

Figure 2. Luminescence signal of $Ru(bpy)_3^{2+}$ (a), $Ru(dmb)_3^{2+}$ (b), $Ru(dmeob)_3^{2+}$ (c), and $Ru(dfmb)_3^{2+}$ (d) in H_2O at 500 nm ($\lambda_{ex} = 388$ nm). Open circles represent the experimental data, and solid lines represent the convoluted fit.

3. Results and Discussion

Homoleptic Series. As shown in Figure 2a, the luminescence decay of the parent $Ru(bpy)_3^{2+}$ complex is quite similar to the IRF (3−5 ps fwhm), indicating that the luminescence observed at 500 nm (20 000 cm^{-1}) vanishes with a time constant much shorter than the resolution of our instrument. The decay traces, $F(t)$, of $Ru(bpy)_3^{2+}$ and its derivatives were fit by iterative reconvolution of the IRF, $g(t)$, with a decay function, $f(t)$ (eqs 1 and 2):

$$F(t) = \int_{-\infty}^{t} g(t')f(t - t')\,dt' \qquad (1)$$

where

$$f(t) = A_1 \exp(-t/\tau_1) \qquad (2)$$

Repeated measurements gave single-exponential decay functions, $f(t)$, with time constants on the order of 1 ps for $Ru(bpy)_3^{2+}$. Since our streak camera cannot compete with fluorescence upconversion systems in terms of time resolution,[12,20] we infer that the 1-ps time constant we extract mathematically encompasses the 40-fs time constant determined by Bhasikuttan et al. in addition to any vibrational relaxation occurring on the time scale of the excitation pulse (~150 fs). We note that when $Ru(bpy)_3^{2+}$ is excited with 400-nm (~120 fs) excitation, the transient absorption spectrum monitored in the region of the 2,2′-bipyridine radical anion (532 nm) shows biexponential kinetics with time constants on the order of 120 fs and 5 ps; 480 nm (30 fs fwhm) excitation yields only the faster time constant.[21]

Results obtained for various homoleptic ruthenium(II) complexes comprising 4,4-substituted bipyridines were considerably different from those obtained with the parent $Ru(bpy)_3^{2+}$ complex. In particular, the decay kinetics observed at 500 nm for these complexes were best described by a biexponential decay convolved with the IRF (eq 3). Typically, an IRF-limited fast component having a time constant on the order of 1−5 ps (τ_1) was followed by much a slower component ($\tau_2 > 50$ ps) that did not completely decay over the observation window ($\Delta t \approx$ 300 ps, jitter-free trigger unit). The traces for $Ru(dmb)_3^{2+}$, $Ru(dmeob)_3^{2+}$, and $Ru(dfmb)_3^{2+}$ are compared to that of the parent $Ru(bpy)_3^{2+}$ in Figure 2. Using a slow sweep unit to trigger the streak camera, we determined the longer lifetimes to be 1−3 ns.[22]

$$f(t) = A_1 \exp(-t/\tau_1) + A_2 \exp(-t/\tau_2) \qquad (3)$$

To derive a plausible kinetic model to describe the observed dynamics, it is necessary to speculate on the origin of the multiexponential decay at 500 nm (20 000 cm^{-1}). Two important aspects that are not addressed in this report include resolution of the IRF-limited decay in the luminescence experiments and transient absorption data. While the transient absorption experiments will be disclosed in a separate report, we are at the limit of the time resolution available with our currect streak camera setup for emission measurements. In the absence of these data, several assumptions must be made with respect to the number of processes represented by τ_1 and their relative energies.

Our first assumption is that we are, indeed, exciting a ^{1}MLCT transition and that subsequent dynamics involve orbitals of similar parentage. While ^{1}MC states are thought to lie near 395 nm (25 300 cm^{-1}), direct absorption to these states are Laporte-forbidden[7,9] and should contribute very little to the overall absorption near 388 nm (25 800 cm^{-1}). Therefore, excitation at this wavelength populates a state that is prodominantly singlet in character, most likely $^1A_2(d\pi_e \rightarrow \pi_e^*)$, which has been both predicted and observed.[23−25] On the basis of the time scale for the formation of the lowest-energy ^{3}MLCT state in $Ru(bpy)_3^{2+}$, population of the ^{3}MC manifold from this F−C ^{1}MLCT state is assumed to be negligible.

(20) Asbury, J. B.; Ellingson, R. J.; Ghosh, H. N.; Ferrere, S.; Nozik, A. J.; Lian, T. *J. Phys. Chem. B* **1999**, *103*, 3110−3119.

(21) Damrauer, N. H.; McCusker, J. K. *J. Phys. Chem. A* **1999**, *103*, 8440−8446.

(22) It is worth noting the possibility of impurities giving rise to nonexponential kinetics, a problem that has plagued others in the field of ruthenium polypyridyl photophysics. While various chromatographic and steady-state spectroscopic techniques were employed to ensure samples of high purity, time-resolved emission data were acquired at multiple wavelengths. Multiexponential decays with similar time constants were observed at both 475 and 520 nm. Beyond ~530 nm, interference from the long-lived ^{3}MLCT state ($\lambda_{max} = 610$ nm) prevented multiwavelength analyses. The low quantum yield of the state giving rise to emission at 500 nm ($\Phi <$ 1E−04) makes multiwavelength analysis of the luminescence profile somewhat difficult; however, the data we do have suggest the presence of one emitting species. In addition, these nonexponential kinetics are observed immediately upon laser irradiation, indicating that laser-induced sample degradation is not a factor. Further substantiating this conclusion, identical results were obtained using both the Cl^- salts of the complexes in H_2O and the PF_6^- salts in MeCN.

(23) Daul, C.; Baerends, E. J.; Vernooijs, P. *Inorg. Chem.* **1994**, *33*, 3538−3543.

(24) Felix, F.; Ferguson, J.; Guedel, H. U.; Ludi, A. *J. Am. Chem. Soc.* **1980**, *102*, 4096−4102.

(25) Ferguson, J.; Krausz, E.; Vrbancich, J. *Chem. Phys. Lett.* **1986**, *131*, 463−467.

Our second assumption involves the kinetic pathway leading from the initially excited F−C state to the state(s) being probed at 500 nm (20 000 cm^{-1}) in our experiments. Since a large number of spin−orbit coupled states lies between 380 and 500 nm (26 000−19 800 cm^{-1}),[23,26,27] it is conceivable that the wave packet samples more than one electronic surface before reaching the state(s) responsible for the observed emission at 500 nm (20 000 cm^{-1}). The absence of simple cascade population dynamics in transition metal complexes[18] means that the observed dynamics occurring on any lower surface will be a function of the state(s) initially populated. This concept has been demonstrated by Damrauer et al. wherein the absorption of the bpy and dmb radical anions (in $Ru(bpy)_3^{2+}$ and $Ru(dmb)_3^{2+}$) displays biexponental kinetics when pumped at 400 nm and monoexponential kinetics when pumped at 480 nm. In these cases, ∼120-fs time resolution was sufficient to discern such discrepancies; by limiting our experiments to ∼3-ps resolution, we assume that all information concerning the initial population of the state giving rise to weak emission near 500 nm (20 000 cm^{-1}) is contained within the IRF-limited decay, τ_1 (i.e., kinetics slower than the IRF do not reflect differential rise times of the 500-nm state from higher-lying states).

On the basis of these assumptions and the ultrafast dynamics that have been established for $Ru(bpy)_3^{2+}$ and $Ru(dmb)_3^{2+}$, we infer that the 1−5-ps (τ_1) components in our experiments reflect contributions from the ^{1}MLCT−^{3}MLCT surface crossings (and possibly vibrational cooling). Time constants for these processes in addition to vibrational cooling on the ^{3}MLCT surface have been measured by others;[12−21] our experiments do not probe the hot band-to-hot band emission observed near 620 nm (16 100 cm^{-1}) in Bhasikuttan's measurements. However, in the case of $Ru(dmb)_3^{2+}$ (and the other 4,4-homoleptic complexes), we observe an additional component at 500 nm (20 000 cm^{-1}), τ_2, which is not evident in previous transient absorption or fluorescence upconversion measurements. Therefore, existing kinetic models must be adjusted to incorporate another non-thermalized state that is also capable of repopulating the ground state via direct photon emission.

The availability of transient absorption data for $Ru(dmb)_3^{2+}$ at 400 nm makes this member of the series a reasonable starting point for understanding the slower kinetics resulting from higher energy excitation. To reiterate, 400-nm excitation of $Ru(dmb)_3^{2+}$ results in the biexponential decay of $dmb^{+\bullet}$ (532 nm), formed by the charge-transfer transition.[21] According to Damrauer et al., the dynamics occurring on the time scale of the excitation pulse (120 fs) include contributions from the ^{1}MLCT−^{3}MLCT surface crossing while the 5-ps decay reflects vibrational cooling dynamics in the ^{3}MLCT excited state; no further changes are observed after $t = 15-20$ ps. This constant signal at longer time delays contrasted with our observation of τ_2 emission (500 nm) ($\lambda_{ex} = 388$ nm) indicates that the pump wavelength must influence the number of states that the wave packet samples following excitation.

Following the kinetic model proposed by Bhasikuttan et al. for $Ru(bpy)_3^{2+}$ (which does not incorporate τ_2), we assign τ_2 as emission from state C (Figure 3), where state A corresponds to the ^{1}MLCT manifold and state B represents the corresponding triplet manifold. In this context, state C could be a higher

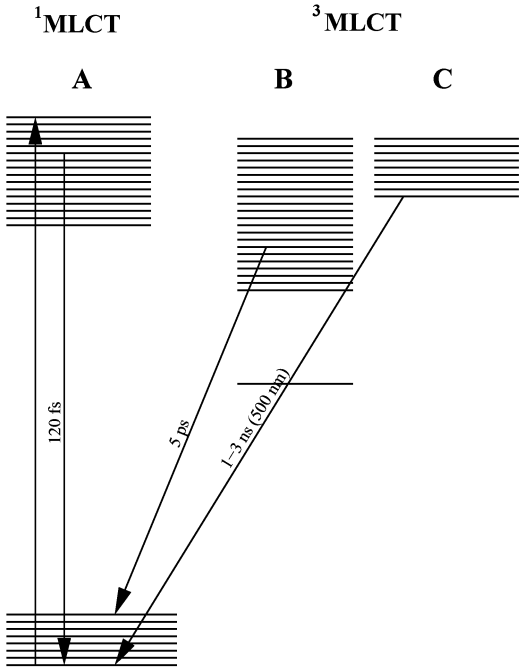

Figure 3. Jablonski diagram for $Ru(dmb)_3^{2+}$ modified to include τ_2.

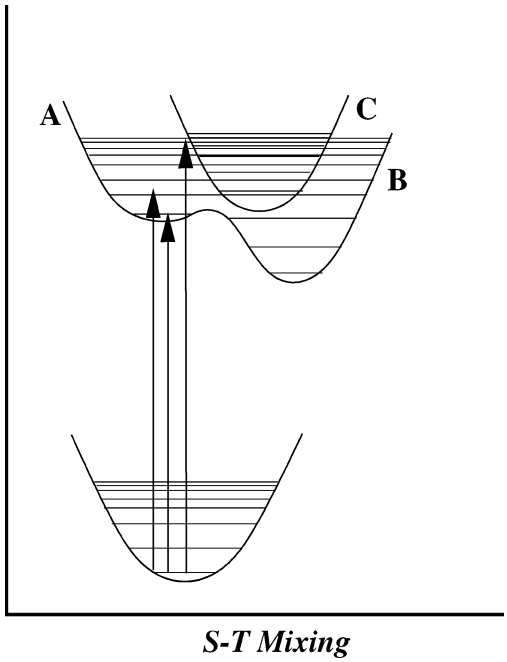

Figure 4. PES diagram depicting the influence of excitation energy on population dynamics where the abscissa indicates the degree of $S-T$ mixing.

vibrational level of state B, a local minimum on the potential energy surface of state B, or a distinct state altogether. If state C were, indeed, a "hot" vibrational state of B, then τ_2 would be expected to be much shorter since vibrational cooling is generally on the order of 0.5−5 ps. Therefore, only the latter two possibilities are considered further.

Figure 4 provides a qualitative picture of the effect of excitation wavelength on the state(s) initially populated and, thus, the origin of τ_2. While state C is depicted as a distinct electronic state, its presence as another local minimum on the A−B surface cannot be discounted. In either case, it is envisioned that 388-nm excitation populates some "upper"

(26) Waterland, M. R.; Kelley, D. F. *J. Phys. Chem. A* **2001**, *105*, 4019−4028.
(27) Houten, J. V.; Watts, R. J. *J. Am. Chem. Soc.* **1976**, *98*, 4853−4858.

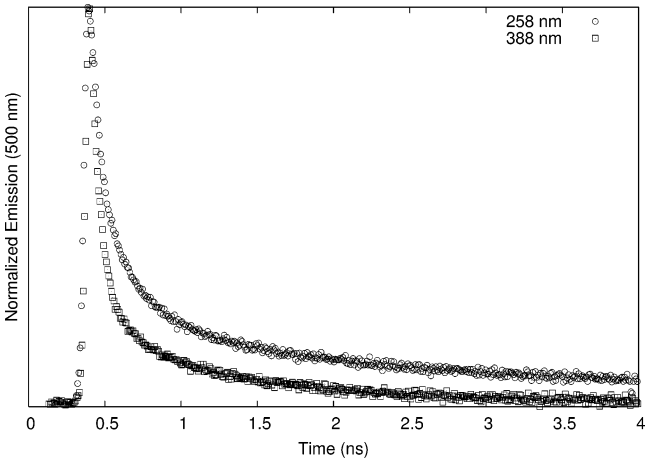

Figure 5. Excitation wavelength dependence for the 500-nm emission of $Ru(dmeob)_3^{2+}$.

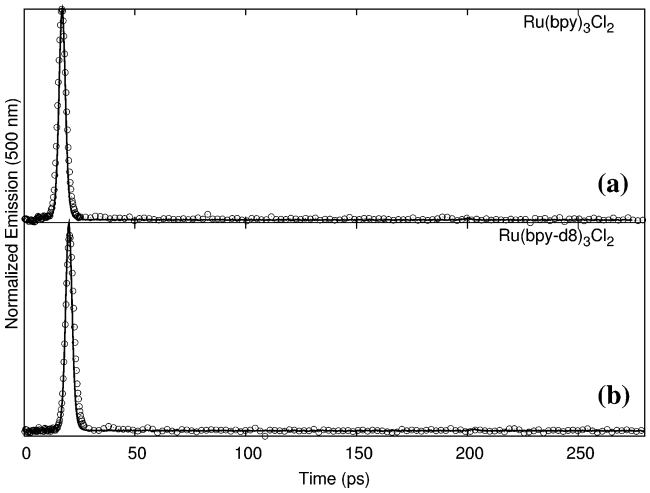

Figure 6. Luminescence signal of $Ru(bpy)_3^{2+}$ (a) and $Ru(bpy\text{-}d8)_3^{2+}$ (b) in H_2O at 500 nm ($\lambda_{ex} = 388$ nm). Open circles represent the actual data, and solid lines represent the IRF.

vibrational level of the singlet manifold that is capable of accessing states A, B, and C. In this scenario, τ_1 encompasses fluorescence from the F−C state, ISC to states B and C, and possibly IVR/IC in the singlet manifold; τ_2 encompasses luminescence from state C and any competing nonradiative deactivation processes. As the excitation energy is attenuated, access to state C is prohibited, and τ_1 contains ISC to state B only in addition to any competing IVR/IC. What is not emphasized in Figure 4 but should be mentioned is that a shift to longer wavelength excitation could prevent population of the upper vibrational levels in state B that give rise to the hot band-to-hot band emission (620 nm) observed by Bhasikuttan et al. This explanation also accounts for the discrepancy in the decay kinetics (532 nm) observed in the transient absorption spectra of $Ru(bpy)_3^{2+}$ and $Ru(dmb)_3^{2+}$ when the pump wavelength is changed.[18,21]

While it is convenient to compare our results produced from 388-nm excitation with literature results produced from longer wavelength excitation in order to construct a picture of the excited-state dynamics, it is ideal to have access to multiple excitation wavelengths under the same experimental conditions. Unfortuntely, we were not able to tune our excitation source to longer wavelengths without a significant attenuation of power.[28] When measuring luminescence with quantum yields on the order of $\leq 10^{-4}$, this power loss is not acceptable. Therefore, we frequency-tripled the excitation beam and tested our proposed model with shorter wavelength excitation (258 nm). On going from 388 to 258 nm excitation, the amplitude and lifetime associated with τ_2 for the various homoleptic complexes increased as demonstrated for $Ru(dmeob)_3^{2+}$ in Figure 5. In fact, $Ru(bpy)_3^{2+}$, showing no evidence of the decay process represented by τ_2 at $\lambda_{ex} = 388$ nm, displays a small contribution from τ_2 when irradiated at 258 nm.

Not all of the homoleptic complexes studied produced the prominent longer-lived component. While a recent report suggested the presence of a substantial deuterium isotope effect on the luminescence lifetime of $Ru(bpy)_3^{2+}$ at 500 nm (20 000 cm^{-1}),[13,29] we saw no evidence of this effect upon monitoring the luminescence of perdeuterated $Ru(bpy)_3^{2+}$ at 500 nm over a 300-ps time window (Figure 6). If deuterium substitution does, indeed, enhance the luminescence lifetime, this enhancement still does not extend the lifetime beyond our IRF of 3 ps. It should be noted that, in some cases, luminescence of perdeuterated $Ru(bpy)_3^{2+}$ was observed at 500 nm at times beyond 20 ns. However, in these cases, samples of perdeuterated $Ru(bpy)_3^{2+}$ had been stored in aqueous solution for extended periods of time. All freshly prepared samples gave IRF-limited decays at 500 nm.

As for perdeuterated $Ru(bpy)_3^{2+}$, 5,5′-substitution in $Ru(dfmb)_3^{2+}$ and $Ru(dmb)_3^{2+}$ resulted in the disappearance of τ_2 (Figure S1). Current efforts are focused on determining whether the change from 4,4′- to 5,5′-substitution results in instrument response limited vibrational cooling or whether this kinetic pathway disappears completely. Any explanation must consider electronic factors since the static measurements reveal that both the F−C state and the thermally equilibrated ^{3}MLCT state of $Ru(d5mb)_3^{2+}$ and $Ru(d5fmb)_3^{2+}$ lie at higher energy relative to their 4,4′-counterparts. However, vibrational factors cannot be neglected since complexes exhibiting similar static and nanosecond properties (i.e., $Ru(bpy)_3^{2+}$ and $Ru(dfmb)_3^{2+}$) differ drastically in their picosecond dynamics.

Heteroleptic Series. To determine the role that symmetry plays in the appearance of τ_2, we investigated a series of heteroleptic complexes. The picosecond luminescence spectra of several heteroleptic complexes of the type $Ru(LL)_2(LL')$ (where LL = bpy, dfmb, or d5fmb and LL′ = dmb, d5mb, dmeob, or bpy) are appended in the Supporting Information (Figures S2 and S3). When LL = bpy, the luminescence decay measured at 500 nm (20 000 cm^{-1}) was ≪5 ps regardless of the identity of LL′. Interestingly, the mixed heteroleptic complexes where LL and LL′ are any combination of the 4,4′-substituted bipyridines did not give rise to the prominent τ_2 component characteristic of the picosecond biexponental kinetics observed in the corresponding homoleptic complexes. While this finding was quite surprising and remains puzzling, current efforts are directed at understanding the requirement of 4,4′-substitution and D_3 symmetry for τ_2 to make a noticeable contribution to the observed kinetics.

(28) The power output of the OPA is on the order of 5−10 mW.
(29) Browne, W. R.; Coates, C. G.; Brady, C.; Matousek, P.; Towrie, M.; Botchway, S. W.; Parker, A. W.; Vos, J. G.; McGarvey, J. J. *J. Am. Chem. Soc.* **2004**, *126*, 10190.

4. Concluding Remarks

In conclusion, we have probed the picosecond dynamics at 500 nm (20 000 cm^{-1}) of a series of $Ru(bpy)_3^{2+}$ derivatives using 388-nm excitation. Luminescence from nonthermalized excited states has been measured for the series and found to exhibit no discernible deuterium isotope effect on this time scale. While this is in disagreement with the prediction of others, we acknowledge the sensitivity of these dynamics to both pump and probe wavelengths. We did, however, find longer-lived emission (>50 ps) among the series of 4,4′-substituted homoleptic complexes, not unlike that which was erroneously reported for $Ru(bpy\text{-}d8)_3^{2+}$. This second component was not prominent in the heteroleptic series nor did it make a significant contribution in the 5,5′-substituted complexes. In the absence of a slow component to the rise time measured for the thermalized ^{3}MLCT, we concluded that these slower kinetics exhibited by the 4,4′-substituted homoleptic complexes are most likely associated with a higher-lying electronic state on the triplet surface that is not sampled when longer excitation wavelengths are employed.

We feel that our results should be disclosed at this stage to generate interest in the ultrafast dynamics of these $Ru(bpy)_3^{2+}$ derivatives and to emphasize the importance of excitation energy on the observed kinetics. This work provides further evidence that the efficiency of ISC to thermalized ^{3}MLCT state(s) for $Ru(bpy)_3^{2+}$ (and some of its derivatives) is not unity, as routinely stated prior to the work of Bhasikuttan et al. Perhaps more importantly, it implicates a distinct nonthermalized state, thought to be of triplet origin, that may be involved in photoinduced dye-to-semiconductor electron injection. As demonstrated by our preliminary studies on the heteroleptic series and the 5,5′-substituted homoleptic complexes, the population of this state can be controlled by varying both ligand identity and the substitution position on the bipyridine ring. This sort of control over processes in the nonergodic regime is crucial to the rational design and development of photovoltaic dye-sensitized devices, and current endeavors are underway to further elucidate the dynamics of this nonthermalized state.

Acknowledgment. F.L.C. and N.P.S. gratefully acknowledge the Canadian Foundation for Innovation (CFI) and the Natural Science and Engineering Research Council of Canada (NSERC) for financial support of this research. K.A.W.Y.C. and F.S.L. thank NSERC, the Izaak Walton Killam Memorial Foundation, and the Walter C. Sumner Foundation for postgraduate scholarships. S.A.M. thanks D. Magde for insightful discussions. We also thank B. Millier for supplying his electronic expertise.

Supporting Information Available: Additional synthetic and time-resolved spectroscopic data. This material is available free of charge via the Internet at http://pubs.acs.org.

JA0461872